

## A Stiboranyl Platinum Triflate Complex as an Electrophilic Catalyst

Di You, Jesse E. Smith, Srobona Sen, and François P. Gabbaï\*

Cite This: <https://dx.doi.org/10.1021/acs.organomet.0c00193>

Read Online

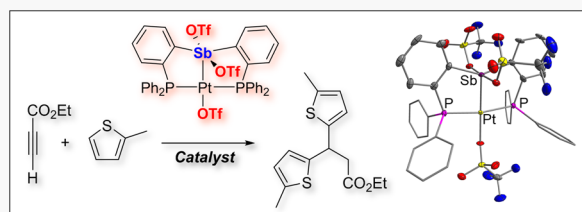
ACCESS |

Metrics &amp; More

Article Recommendations

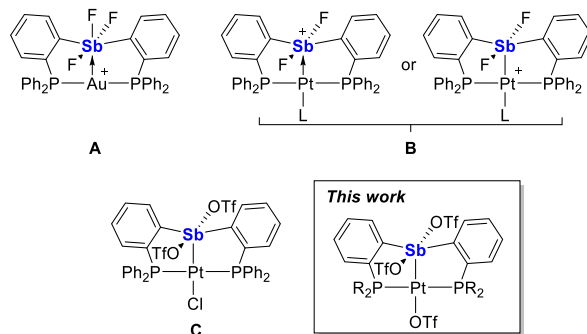
Supporting Information

**ABSTRACT:** With the view of developing electrophilic late-transition-metal catalysts, we have now synthesized  $[(o\text{-}(Ph_2P)C_6H_4)_2Sb(OTf)_2]Pt(OTf)$  (2) and  $[(o\text{-}(^iPr_2P)C_6H_4)_2Sb(OTf)_2]Pt(OTf)$  (4) by treatment of the corresponding trichlorides ( $[(o\text{-}(R_2P)C_6H_4)_2SbCl_2]PtCl$  ( $R = Ph$ ,  $^iPr$ )) with 3 equiv of  $AgOTf$ . The crystal structures of 2 and 4 confirmed that the chloride ligands have been fully substituted by more labile triflate ligands. Despite structural similarities in the dinuclear cores of 2 and 4, only 2 acts as a potent carbophilic catalyst in enyne cyclization reactions. The high activity of 2 is also reflected by its ability to promote the addition of pyrrole and thiophene derivatives to alkynes. Structural and computational analyses suggest that the superior reactivity of 2 results from both favorable steric and electronic effects. Finally, a comparison of 2 with the previously reported self-activating catalyst  $[(o\text{-}(Ph_2P)C_6H_4)_2Sb(OTf)_2]PtCl$  underscores the benefits of triflate for chloride substitution.



Antimony(V) derivatives are powerful Lewis acids which have been used for the generation of superacids<sup>1,2</sup> or as catalysts for transformations that necessitate strong electrophilic activation.<sup>3,4</sup> While antimony(V) halides have been at the forefront of this chemistry for much of the past half century, recent efforts have shown that organoantimony compounds, which are more convenient to handle than their halide counterparts, also display appealing Lewis acidic properties.<sup>5–11</sup> These advantageous properties have come to light in the development of applications in organic reaction catalysis<sup>12–16</sup> and anion sensing.<sup>17–20</sup> With the view of interfacing Lewis acidic antimony moieties with transition metals, several groups have recently investigated the synthesis of complexes in which the main-group element and the metal either are directly connected<sup>21–24</sup> or held in close proximity by auxiliary ligands.<sup>25–28</sup> Examples of such complexes include A and B, two compounds in which the high Lewis acidity of the antimony center defines the catalytic properties of the late-transition-metal center (Chart 1).<sup>26,29</sup> In these complexes, we proposed that the  $\sigma$ -accepting properties of the antimony moiety serve to activate the late-transition-metal center via formation of a  $M\rightarrow Sb$  interaction, leading to an enhancement in the carbophilic reactivity of the metal center. In a separate investigation, we reported an antimony platinum complex (C) in which the presence of two triflate anions accentuated the Lewis acidity of the stiboranyl moiety.<sup>30</sup> Despite the apparent coordinative saturation of the platinum center, we observed that this compound was a self-activating catalyst for enyne cyclization and hydroarylation reactions (Chart 1). We speculated that this complex owes its catalytic activity to the presence of a Lewis acidic antimony center which helps activate the Pt–Cl bond intramolecularly, allowing for substrate activation. Intending to further enhance the unique

**Chart 1. Examples of Gold–Antimony and Platinum–Antimony Complexes Previously Used as Electrophilic Catalysts<sup>a</sup>**



<sup>a</sup>The inset shows the type of structure targeted in this study.

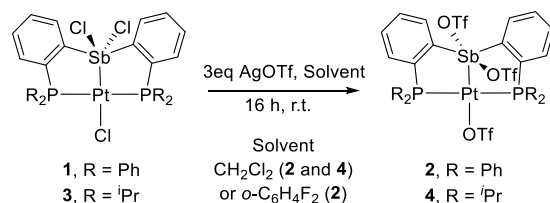
properties of such platforms, we have now targeted an analogue of C in which the chloride ligand bound to platinum is also replaced by a more weakly coordinating triflate anion. Given the lability of the triflate anions, we speculated that such a complex might generate an exposed platinum species, the reactivity of which would be further enhanced by the presence of an adjacent electrophilic antimony triflate unit.

**Special Issue:** Organometallic Chemistry of the Main-Group Elements

**Received:** March 22, 2020

While we anticipated that exchange of the platinum-bound chloride anion of **C** might be difficult, we observed that the reaction of the known complex  $[(o\text{-}(Ph_2P)C_6H_4)_2SbCl_2]PtCl$  (**1**)<sup>31</sup> with 3 equivalents of AgOTf proceeded smoothly to afford the target complex  $[(o\text{-}(Ph_2P)C_6H_4)_2SbOTf_2]PtOTf$  (**2**) (Scheme 1). The same reaction was also carried out with

**Scheme 1. Synthesis of 2 and 4**

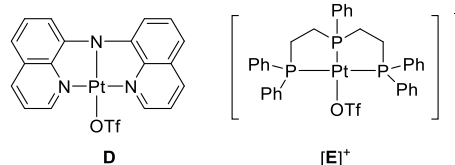


$[(o\text{-}(iPr_2P)C_6H_4)_2SbCl_2]PtCl$  (**3**), the isopropyl analogue of **1** which was newly synthesized for this study. Again, we observed facile substitution of the three chloride anions when 3 equiv of AgOTf were employed, leading to the formation of  $[(o\text{-}(iPr_2P)C_6H_4)_2SbOTf_2]PtOTf$  (**4**). The triflate derivatives **2** and **4** have been isolated as moisture-sensitive solids. Their <sup>31</sup>P NMR spectra feature single resonances at 49.4 ppm for **2** and 73.9 ppm for **4** that are respectively coupled to the <sup>195</sup>Pt nuclei by <sup>1</sup>J<sub>Pt-P</sub> = 2450 and 2383. These values are close to those measured for **1** (<sup>1</sup>J<sub>Pt-P</sub> = 2566 Hz) and **3** (<sup>1</sup>J<sub>Pt-P</sub> = 2473 Hz).

Single crystals of the tris(triflate) complexes could be easily obtained upon diffusion of pentane into a *o*-C<sub>6</sub>H<sub>4</sub>F<sub>2</sub> or CH<sub>2</sub>Cl<sub>2</sub> solution of the complex for **2** and **4**, respectively. Compound **2**, which crystallizes with interstitial *o*-C<sub>6</sub>H<sub>4</sub>F<sub>2</sub> molecules, features two molecules of the complex in the asymmetric unit. These two molecules, arbitrarily referred to as *molecule a* and *molecule b*, feature very similar structures. The geometry about the dinuclear core of these two independent molecules is also very similar to that of **4**, as illustrated hereafter. In both **2** and **4**, two triflate anions are bound to the antimony center. The resulting Sb–O<sub>triflate</sub> distances in **2** (2.201(6)–2.246(6) Å) and **4** (2.199(2)–2.211(2) Å) fall within a rather narrow range and are comparable to those measured in complex **C** (2.189(3)–2.219(3) Å), indicating that the triflate anions are tightly coordinated to the antimony atom. As in complex **C**, the antimony atoms of **2** and **4** adopt a distorted-trigonal-bipyramidal geometry in which the two triflate anions occupy axial positions, as indicated by the O<sub>triflate</sub>–Sb–O<sub>triflate</sub> angles of 177.0(2)° for *molecule a* of complex **2**, 178.4(2)° for *molecule b* of complex **2**, and 176.41(6)° for complex **4**. The largest distortion occurs in the equatorial plane as indicated by the C–Sb–C angles of 145.5(3)° for *molecule a* of complex **2**, 144.8(3)° for *molecule b* of complex **2**, and 143.52(10)° for **4** which are notably larger than the ideal value of 120°. The Sb–Pt distances in **2** (2.4118(6) Å for *molecule a* and 2.4106(6) Å for *molecule b*) and **4** (2.4237(12) Å) are shorter than those in complex **1** (2.4407(5) Å) and **3** (2.4467(10) Å), indicating a contraction of the Sb–Pt core triggered by electron depletion. This notion is supported by a search of the Cambridge Structural Database, which indicates that these Sb–Pt bond distances are among the shortest for complexes featuring this linkage.<sup>28,32–34</sup> The platinum-bound triflate anions form Pt–O<sub>triflate</sub> bonds of 2.130(5) and 2.122(6) Å for *molecules a* and *b* of complex **2**, respectively. These Pt–O<sub>triflate</sub> bond distances are slightly shorter than that in **4** (2.168(2) Å), which may indicate that the electrophilicity of the platinum center in **4** is

reduced by the more electron-releasing diisopropylphosphino groups. Finally, we will note that platinum triflate complexes have been previously structurally characterized, as in the case of **D** and **E**, which possess Pt–O<sub>triflate</sub> bonds of 2.097(2) and 2.102(9) Å, respectively (Chart 2).<sup>35,36</sup>

**Chart 2. Examples of Platinum Triflate Complexes**



The structures of **2** and **4** have been studied computationally, and some of their bonding features were examined using the natural bond orbital (NBO) method. Examination of the NBO output indicates that the Sb–Pt bonds in **2** and **4** are covalent (Figure 1 and Figure S18). Indeed, the corresponding

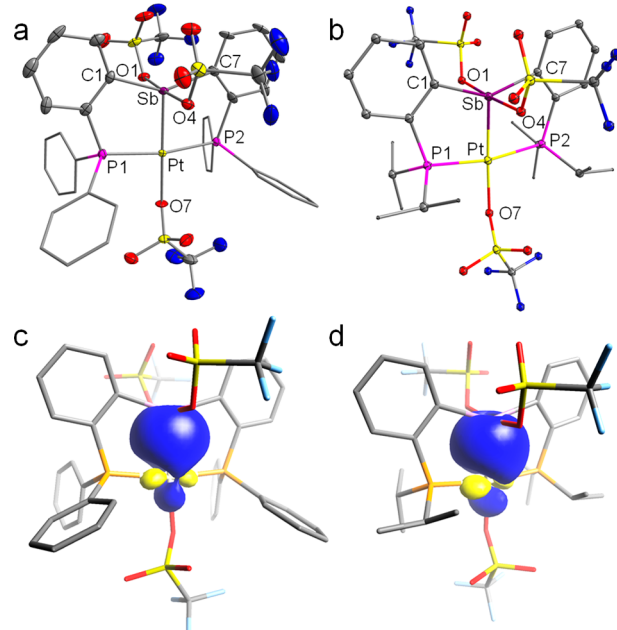


**Figure 1.** (top) Solid-state structures of **2** (a) and **4** (b). Thermal ellipsoids are drawn at the 50% probability level. Phenyl and isopropyl groups are drawn in wireframe. Hydrogen atoms are omitted for clarity. For **2**, only one of the two independent molecules is shown and the interstitial solvent molecules are omitted. (bottom) NLMO plot (isosurface value 0.04) of the major Sb–Pt bonding interactions in **2** (c) and **4** (d).

natural localized molecular orbitals (NLMOs) show that the antimony and platinum atoms both contribute to the Sb–Pt bond (Sb 56.97% and Pt 38.20% for **2**; Sb 56.45% and Pt 38.77% for **4**). The lack of strong polarization in the Sb–Pt bond is a feature that these new complexes share with their trichloride precursors **1** and **3** as well as complex **C**.<sup>30</sup> The natural population analysis (NPA) charge reveals that the platinum atoms in **2** (0.278) and **4** (0.266) are more positive than those in **1** (0.167) and **3** (0.163). The higher NPA charge observed for the tris(triflate) complex is ascribed to the weak coordination of nature of the triflate anions, making the core of the complexes more exposed and electron deficient.

Given the known lability of the triflate ligand, we speculated that **2** and **4** might behave as electrophilic platinum catalysts.<sup>37–42</sup> To test this possibility, we became eager to investigate the use of these two complexes in the cycloisomerization of 2-allyl-2-(2-propynyl)malonate (Table 1), a

**Table 1. 1,6-Enyne Cyclization Catalysis**

entry	cat.	time	conversion <sup>a</sup> (%)
			5 mol% Cat.
1	C	3.5 h	96
2	<b>2</b>	10 min	96
3	<b>4</b>	3 h	0

<sup>a</sup>Conversion determined by <sup>1</sup>H NMR.

reaction often used to benchmark the activity of late-transition-metal catalysts. Complex **2** proved to be remarkably active. Indeed, when **2** was used at a 5 mol % loading, the cycloisomerization reached completion within 10 min when it was carried out at room temperature (Table 1, entry 2). The same reaction took 3.5 h to complete when **C** was employed as a catalyst (Table 1, entry 1). The contrasting activity of these two catalysts underscores the benefit of substituting the platinum-bound chloride ligand of **1** with the more weakly coordinating triflate anion in **2**. We propose that the increased lability of the triflate anion increases accessibility of the platinum center by the reaction substrate, leading to a more efficient catalyst.

To our surprise, we found that **4** was inactive as a catalyst for this reaction. An initial factor that may contribute to this lack of activity is the lower NPA charge of the platinum atom of **4** (0.266 vs 0.278 in **2**), which suggests that the catalytic activity of **4** may be negatively affected by the more donating isopropyl-substituted phosphino groups. The lack of catalytic activity of this complex may also originate from steric effects imposed by the bulkier isopropyl groups, which lead to a less accessible platinum center. To support this argument, we inspected the steric maps of the ligands in both complexes, as shown in Figure 2.<sup>43</sup> Comparison of the topographic steric

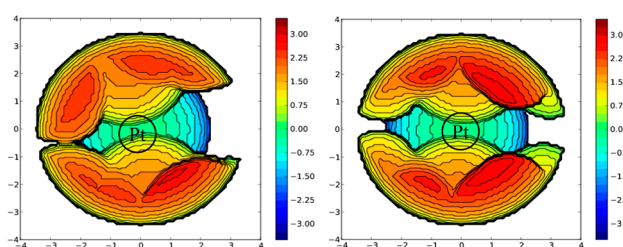


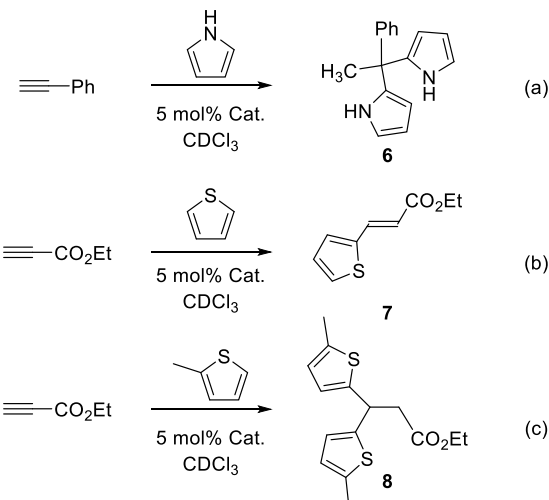
**Figure 2.** Topographic steric maps of the phosphino-antimony ligands in **2** (left) and **4** (right). The red and blue zones indicate the more and less hindered zones in the catalytic pocket, respectively.

maps identifies some important differences in the shapes of the catalytic pockets of the two complexes. The %V<sub>Bur</sub> (percent buried volume) at platinum in **4** (72.2%) is clearly larger than that in **2** (69.1%), suggesting greater accessibility in the latter. Such steric effects have been previously discussed in the case of the related gold antimony complexes  $[(o\text{-}(\text{Pr}_2\text{P})\text{C}_6\text{H}_4)_2(o\text{-C}_6\text{Cl}_4\text{O}_2)\text{SbPh}\text{Au}]^+$  and  $[(o\text{-}(\text{Ph}_2\text{P})\text{C}_6\text{H}_4)_2(o\text{-C}_6\text{Cl}_4\text{O}_2)\text{SbPh}\text{Au}]^+$ .

Indeed, while the former displayed no carbophilic reactivity, the latter readily promoted the cycloisomerization of *N*-(prop-2-yn-1-yl)benzamide or the addition reaction of *p*-toluidine to phenylacetylene. No further attempts to use **4** as a catalyst were considered.

We have also probed the use of **2** as a catalyst for the addition of heteroaryls to alkynes. The reaction of pyrrole with phenylacetylene was investigated first, using  $\text{CDCl}_3$  as a solvent and a 5 mol % catalyst loading. The progress of the reaction was monitored by <sup>1</sup>H NMR spectroscopy, and the results are summarized in Table 2. As anticipated from the reactivity

**Table 2. Addition of Pyrrole and Thiophenes to Alkynes Catalyzed by **2** and **C****



entry	cat.	reacn	time	temp (°C)	product	yield (%)
1	<b>C</b>	(a)	12 h	25	<b>6</b>	68 <sup>a</sup>
2	<b>2</b>	(a)	10 min	25	<b>6</b>	89 <sup>a</sup>
3	<b>C</b>	(b)	19 h	60	<b>7</b>	<10 <sup>a</sup>
4	<b>2</b>	(b)	16 h	60	<b>7</b>	87 <sup>b</sup>
5	<b>C</b>	(c)	7 h	60	<b>8</b>	19 <sup>a</sup>
6	<b>2</b>	(c)	7 h	60	<b>8</b>	76 <sup>a</sup>

<sup>a</sup>Conversion determined by <sup>1</sup>H NMR spectroscopy. <sup>b</sup>Isolated yield.

pattern observed in the cycloisomerization of 2-allyl-2-(2-propynyl)malonate, complex **2** is a very active catalyst which promotes the formation of the double-addition product **6** within minutes. Integration of the <sup>1</sup>H NMR spectrum indicates a 89% conversion, after just 10 min (Table 2, entry 2). Catalyst **C** is also able to promote this reaction, albeit at a much slower rate. While no measurable production formation was observed within the first few minutes of the reaction <sup>1</sup>H NMR monitoring indicated a 68% conversion after 12 h (Table 2, entry 1).<sup>43</sup> The higher reactivity of **2** again illustrates the benefits that result from replacing the platinum-bound chloride ligand of **C** by a triflate ligand as in **2**.

Finally, in order to benchmark the activity of **2** against more challenging substrates, we have also tested reactions involving thiophenes as the heteroaryl. Thiophenes are among one of the most difficult classes of substrates to activate, as the free electron pair at sulfur can coordinate to the platinum center.<sup>46,47</sup> Because no reaction was observed with phenylacetylene, we decided to use ethyl propiolate, which owing to its greater electron deficiency shows a higher reactivity. In line with the activity observed in the aforementioned reactions,

complex **2** displayed a much higher activity in comparison to **C**. Both catalysts afforded the monoaddition product **7**, which was isolated in 87% yield after 16 h when **2** was employed (Table 2, entry 4). The same reaction with **C** afforded less than a 10% conversion after 19 h (Table 2, entry 3). Interestingly, when the more electron rich 2-methylthiophene was used as the heteroaryl, the double-addition product<sup>48</sup> was formed (Table 2, entries 5 and 6). This difference highlights the greater electron richness and reactivity of 2-methylthiophene as a nucleophile.

In summary, we describe **2**, a new highly electrophilic antimony–platinum complex featuring three triflate ligands to the dinuclear core. This complex, which can be isolated and stored, behaves as an active catalyst for reactions involving alkynes. On the basis of a comparison with other catalysts, we assign the unusual catalytic activity of **2** to the weakly coordinating nature of the triflate ligand which, we propose, facilitates access to a reactive platinum center. The reactivity of such complexes may benefit from the perhalogenation of the phenylene backbone, a direction we plan to investigate in future studies.

## ■ ASSOCIATED CONTENT

### Supporting Information

The Supporting Information is available free of charge at <https://pubs.acs.org/doi/10.1021/acs.organomet.0c00193>.

Additional experimental and computational details (PDF)

Optimized structures (XYZ)

### Accession Codes

CCDC 1991315–1991317 contain the supplementary crystallographic data for this paper. These data can be obtained free of charge via [www.ccdc.cam.ac.uk/data\\_request/cif](http://www.ccdc.cam.ac.uk/data_request/cif), or by emailing [data\\_request@ccdc.cam.ac.uk](mailto:data_request@ccdc.cam.ac.uk), or by contacting The Cambridge Crystallographic Data Centre, 12 Union Road, Cambridge CB2 1EZ, UK; fax: +44 1223 336033.

## ■ AUTHOR INFORMATION

### Corresponding Author

François P. Gabbaï – Texas A&M University, Department of Chemistry, College Station, Texas 77843, United States;  [orcid.org/0000-0003-4788-2998](https://orcid.org/0000-0003-4788-2998); Email: [francois@tamu.edu](mailto:francois@tamu.edu)

### Authors

Di You – Texas A&M University, Department of Chemistry, College Station, Texas 77843, United States

Jesse E. Smith – Texas A&M University, College of Science, College Station, Texas 77843, United States

Srobona Sen – Texas A&M University, Department of Chemistry, College Station, Texas 77843, United States

Complete contact information is available at:

<https://pubs.acs.org/10.1021/acs.organomet.0c00193>

### Author Contributions

D.Y. and J.E.S. synthesized and characterized **2**. D.Y. carried out all catalytic studies. S.S. synthesized and characterized **3** and **4**. F.P.G. directed the study.

### Notes

The authors declare no competing financial interest.

## ■ ACKNOWLEDGMENTS

This work was performed at Texas A&M University with the support of the National Science Foundation (CHE-1856453), the Welch Foundation (A-1423), and Texas A&M University (Arthur E. Martell Chair of Chemistry).

## ■ REFERENCES

- (1) Olah, G. A.; Schlosberg, R. H. Chemistry in super acids. I. Hydrogen exchange and polycondensation of methane and alkanes in  $\text{FSO}_3\text{H-SbF}_5$  ("magic acid") solution. Protonation of alkanes and the intermediacy of  $\text{CH}_5^+$  and related hydrocarbon ions. The high chemical reactivity of "paraffins" in ionic solution reactions. *J. Am. Chem. Soc.* **1968**, *90*, 2726–2727.
- (2) Olah, G. A.; Klopman, G.; Schlosberg, R. H. Super acids. III. Protonation of alkanes and intermediacy of alkanonium ions, pentacoordinated carbon cations of  $\text{CH}_5^+$  type. Hydrogen exchange, protolytic cleavage, hydrogen abstraction; polycondensation of methane, ethane, 2,2-dimethylpropane and 2,2,3,3-tetramethylbutane in  $\text{FSO}_3\text{H-SbF}_5$ . *J. Am. Chem. Soc.* **1969**, *91*, 3261–3268.
- (3) Koppaka, A.; Park, S. H.; Hashiguchi, B. G.; Gunsalus, N. J.; King, C. R.; Konnick, M. M.; Ess, D. H.; Periana, R. A. Selective C–H Functionalization of Methane and Ethane by a Molecular SbV Complex. *Angew. Chem., Int. Ed.* **2019**, *58*, 2241–2245.
- (4) Chitnis, S. S.; Sparkes, H. A.; Annibale, V. T.; Pridmore, N. E.; Oliver, A. M.; Manners, I. Addition of a Cyclophosphine to Nitriles: An Inorganic Click Reaction Featuring Protio, Organo, and Main-Group Catalysis. *Angew. Chem., Int. Ed.* **2017**, *56*, 9536–9540.
- (5) Coughlin, O.; Krämer, T.; Benjamin, S. L. Diverse structure and reactivity of pentamethylcyclopentadienyl antimony(III) cations. *Dalton Trans.* **2020**, *49*, 1726–1730.
- (6) Chitnis, S. S.; Burford, N.; McDonald, R.; Ferguson, M. J. Prototypical Phosphine Complexes of Antimony(III). *Inorg. Chem.* **2014**, *53*, 5359–5372.
- (7) Robertson, A. P. M.; Chitnis, S. S.; Jenkins, H. A.; McDonald, R.; Ferguson, M. J.; Burford, N. Establishing the Coordination Chemistry of Antimony(V) Cations: Systematic Assessment of  $\text{Ph}_3\text{Sb}(\text{OTf})$  and  $\text{Ph}_3\text{Sb}(\text{OTf})_2$  as Lewis Acceptors. *Chem. - Eur. J.* **2015**, *21*, 7902–7913.
- (8) Hirai, M.; Gabbaï, F. P. Lewis acidic stiborafluorenes for the fluorescence turn-on sensing of fluoride in drinking water at ppm concentrations. *Chem. Sci.* **2014**, *5*, 1886–1893.
- (9) Qiu, R.; Chen, Y.; Yin, S.-F.; Xu, X.; Au, C.-T. A mini-review on air-stable organometallic Lewis acids: synthesis, characterization, and catalytic application in organic synthesis. *RSC Adv.* **2012**, *2*, 10774–10793.
- (10) Wade, C. R.; Gabbaï, F. P. Fluoride Anion Chelation by a Bidentate Stibonium–Borane Lewis Acid. *Organometallics* **2011**, *30*, 4479–4481.
- (11) Singhal, K.; Yadav, R. N. P.; Raj, P.; Agarwal, A. K. On the Lewis acidity of tris(pentafluorophenyl)antimony(V) dichloride towards neutral monodentate O, N and S donor ligands. *J. Fluorine Chem.* **2003**, *121*, 131–134.
- (12) Benz, S.; Poblador-Bahamonde, A. I.; Low-Ders, N.; Matile, S. Catalysis with Pnictogen, Chalcogen, and Halogen Bonds. *Angew. Chem., Int. Ed.* **2018**, *57*, 5408–5412.
- (13) Greb, L. Lewis Superacids: Classifications, Candidates, and Applications. *Chem. - Eur. J.* **2018**, *24*, 17881–17896.
- (14) Yang, M.; Tofan, D.; Chen, C.-H.; Jack, K. M.; Gabbaï, F. P. Digging the Sigma-Hole of Organoantimony Lewis Acids by Oxidation. *Angew. Chem., Int. Ed.* **2018**, *57*, 13868–13872.
- (15) Tofan, D.; Gabbaï, F. P. Fluorinated Antimony(V) Derivatives: Strong Lewis Acidic Properties and Application to the Complexation of Formaldehyde in Aqueous Solutions. *Chem. Sci.* **2016**, *7*, 6768–6778.
- (16) Pan, B.; Gabbaï, F. P.  $[\text{Sb}(\text{C}_6\text{F}_5)_4][\text{B}(\text{C}_6\text{F}_5)_4]$ : An Air Stable, Lewis Acidic Stibonium Salt That Activates Strong Element–Fluorine Bonds. *J. Am. Chem. Soc.* **2014**, *136*, 9564–9567.

(17) Park, G.; Brock, D. J.; Pellois, J.-P.; Gabbaï, F. P. Heavy Pnictogenium Cations as Transmembrane Anion Transporters in Vesicles and Erythrocytes. *Chem.* **2019**, *5*, 2215–2227.

(18) Hirai, M.; Myahkostupov, M.; Castellano, F. N.; Gabbaï, F. P. 1-Pyrenyl- and 3-Perylenyl-antimony(V) Derivatives for the Fluorescence Turn-On Sensing of Fluoride Ions in Water at Sub-ppm Concentrations. *Organometallics* **2016**, *35*, 1854–1860.

(19) Wade, C. R.; Ke, I.-S.; Gabbaï, F. P. Sensing of Aqueous Fluoride Anions by Cationic Stibine–Palladium Complexes. *Angew. Chem., Int. Ed.* **2012**, *51*, 478–481.

(20) Chen, C.-H.; Gabbaï, F. P. Fluoride Anion Complexation by a Triptycene-Based Distiborane: Taking Advantage of a Weak but Observable C–H···F Interaction. *Angew. Chem., Int. Ed.* **2017**, *56*, 1799–1804.

(21) Jolleys, A.; Lake, B. R. M.; Krämer, T.; Benjamin, S. L. A Five-Membered PdSb<sub>n</sub> Coordination Series. *Organometallics* **2018**, *37*, 3854–3862.

(22) Plajer, A. J.; Colebatch, A. L.; Rizzuto, F. J.; Pröhlm, P.; Bond, A. D.; García-Rodríguez, R.; Wright, D. S. How Changing the Bridgehead Can Affect the Properties of Tripodal Ligands. *Angew. Chem., Int. Ed.* **2018**, *57*, 6648–6652.

(23) Benjamin, S. L.; Levason, W.; Light, M. E.; Reid, G.; Rogers, S. M. Bromostibine Complexes of Iron(II): Hypervalency and Reactivity. *Organometallics* **2014**, *33*, 2693–2695.

(24) Benjamin, S. L.; Levason, W.; Reid, G.; Warr, R. P. Halostibines SbMe<sub>2</sub>X<sub>2</sub> and SbMe<sub>2</sub>X: Lewis Acids or Lewis Bases? *Organometallics* **2012**, *31*, 1025–1034.

(25) Lo, Y. H.; Gabbaï, F. P. An antimony(V) dication as a Z-type ligand: Turning on styrene activation at gold. *Angew. Chem., Int. Ed.* **2019**, *58*, 10194–10197.

(26) Yang, H.; Gabbaï, F. P. Activation of a Hydroamination Gold Catalyst by Oxidation of a Redox-Noninnocent Chlorostibine Z-Ligand. *J. Am. Chem. Soc.* **2015**, *137*, 13425–13432.

(27) You, D.; Gabbaï, F. P. Tunable  $\sigma$ -Accepting, Z-Type Ligands for Organometallic Catalysis. *Trends Chem.* **2019**, *1*, 485–496.

(28) Furan, S.; Hupf, E.; Boidol, J.; Brünig, J.; Lork, E.; Mebs, S.; Beckmann, J. Transition metal complexes of antimony centered ligands based upon acenaphthyl scaffolds. Coordination non-innocent or not? *Dalton Trans.* **2019**, *48*, 4504–4513.

(29) You, D.; Yang, H.; Sen, S.; Gabbaï, F. P. Modulating the  $\sigma$ -Accepting Properties of an Antimony Z-type Ligand via Anion Abstraction: Remote-Controlled Reactivity of the Coordinated Platinum Atom. *J. Am. Chem. Soc.* **2018**, *140*, 9644–9651.

(30) You, D.; Gabbaï, F. P. Unmasking the Catalytic Activity of a Platinum Complex with a Lewis Acidic, Non-innocent Antimony Ligand. *J. Am. Chem. Soc.* **2017**, *139*, 6843–6846.

(31) Yang, H.; Gabbaï, F. P. Solution and Solid-State Photoreductive Elimination of Chlorine by Irradiation of a [PtSb]<sup>VII</sup> Complex. *J. Am. Chem. Soc.* **2014**, *136*, 10866–10869.

(32) Waterman, R.; Handford, R. C.; Tilley, T. D. Element–Hydrogen Bond Activations at Cationic Platinum Centers To Produce Silylene, Germylene, Stannylene, and Stibido Complexes. *Organometallics* **2019**, *38*, 2053–2061.

(33) Braunschweig, H.; Dewhurst, R. D.; Hupp, F.; Wolf, J. Unprecedented Oxidative Addition and Metal-Only Lewis Pair Chemistry of Antimony Trihalides. *Chem. - Eur. J.* **2015**, *21*, 1860–1862.

(34) Jones, C.; Junk, P. C.; Steed, J. W.; Thomas, R. C.; Williams, T. C. The interaction of 2-arsa- and 2-stiba-1,3-dionato lithium complexes with Group 8–12 metal halides. *J. Chem. Soc., Dalton Trans.* **2001**, 3219–3226.

(35) Annibale, G.; Bergamini, P.; Bertolasi, V.; Cattabriga, M.; Ferretti, V. Preparation, solution behaviour and X-ray crystal structure of [PtOTf(triphos)]OTf. *Inorg. Chem. Commun.* **2000**, *3*, 303–306.

(36) Harkins, S. B.; Peters, J. C. Base-Promoted Benzene C–H Activation Chemistry at an Amido Pincer Complex of Platinum(II). *Organometallics* **2002**, *21*, 1753–1755.

(37) Liberman-Martin, A. L.; Levine, D. S.; Liu, W.; Bergman, R. G.; Tilley, T. D. Biaryl Reductive Elimination Is Dramatically Accelerated by Remote Lewis Acid Binding to a 2,2'-Bipyrimidyl–Platinum Complex: Evidence for a Bidentate Ligand Dissociation Mechanism. *Organometallics* **2016**, *35*, 1064–1069.

(38) Chianese, A. R.; Lee, S. J.; Gagné, M. R. Electrophilic Activation of Alkenes by Platinum(II): So Much More Than a Slow Version of Palladium(II). *Angew. Chem., Int. Ed.* **2007**, *46*, 4042–4059.

(39) Alcarazo, M. Synthesis, Structure, and Applications of  $\alpha$ -Cationic Phosphines. *Acc. Chem. Res.* **2016**, *49*, 1797–1805.

(40) Parson, T. G.; Butikofer, J. L.; Houlis, J. F.; Roddick, D. M. Organometallics in Superacidic Media: Characterization of Remarkably Stable Platinum–Methyl Bonds in HF/SbF<sub>5</sub> Solution. *Organometallics* **2017**, *36*, 136–141.

(41) Vigalok, A. Electrophilic Halogenation–Reductive Elimination Chemistry of Organopalladium and -Platinum Complexes. *Acc. Chem. Res.* **2015**, *48*, 238–247.

(42) Clement, M. L.; Grice, K. A.; Luedtke, A. T.; Kaminsky, W.; Goldberg, K. I. Platinum(II) Olefin Hydroarylation Catalysts: Tuning Selectivity for the anti-Markovnikov Product. *Chem. - Eur. J.* **2014**, *20*, 17287–17291.

(43) Falivene, L.; Cao, Z.; Petta, A.; Serra, L.; Poater, A.; Oliva, R.; Scarano, V.; Cavallo, L. Towards the online computer-aided design of catalytic pockets. *Nat. Chem.* **2019**, *11*, 872–879.

(44) Sen, S.; Ke, I.-S.; Gabbaï, F. P. T-Shaped Gold→Stiborane Complexes as Carbophilic Catalysts: Influence of the Peripheral Substituents. *Organometallics* **2017**, *36*, 4224–4230.

(45) Oyamada, J.; Kitamura, T. Pt(II)-catalyzed hydroarylation reaction of alkynes with pyrroles and furans. *Tetrahedron* **2009**, *65*, 3842–3847.

(46) Hashmi, A. S. K.; Yang, W.; Rominger, F. Gold(I)-Catalyzed Rearrangement of 3-Silyloxy-1,5-enynes: An Efficient Synthesis of Benzo[b]thiophenes, Dibenzothiophenes, Dibenzofurans, and Indole Derivatives. *Chem. - Eur. J.* **2012**, *18*, 6576–6580.

(47) Hashmi, A. S. K.; Schäfer, S.; Bats, J. W.; Frey, W.; Rominger, F. Gold Catalysis and Chiral Sulfoxides: Enantioselective Synthesis of Dihydroisoindol-4-ols. *Eur. J. Org. Chem.* **2008**, *2008*, 4891–4899.

(48) Kitamura, T.; Mizuhara, T.; Keita, M. L.; Oyamada, J. A Convenient Synthesis of 3,3-Bis(thienyl)propionic Acids by Platinum (II)-Catalyzed Reaction of Thiophenes with Propiolic Acids. *Phosphorus, Sulfur Silicon Relat. Elem.* **2010**, *185*, 1154–1161.